that this assumption is not valid as was already demonstrated by the much higher R and R_w values.

As there were still small residual peaks in residual density maps after the refinement assuming the high-spin state, the electron populations of t_{2g} and e_g orbitals were refined by the least-squares procedure. The difference Fourier maps after this refinement are shown in Figs. 4(*a*) and 4(*b*).* Compared wtih Figs. 2(*a*) and 2(*b*), however, no significant changes are found in these maps. The number of electrons in each orbital is also equal to that of the high-spin state within the experimental errors. Accordingly, the real electronic state of the Fe^{2+} ion in $KFeF_3$ is considered to have the high-spin electron configuration $(t_{2g})^4(e_g)^2$.

Around the F^- ion four positive peaks with heights of 0·21 e Å^{-3} are observed at about 0·2 Å from the F^- nucleus in the directions perpendicular to the Fe–F bond. It is likely that these peaks appeared due to the anharmonic thermal vibration of the F^- ion, because similar but slightly larger peaks were observed around the F^- ion in the deformation density map of $KMnF_3$ crystals, which show a phase transition related to vibration of the F^- ion at 187 K. The thermal parameters of the F^- ion in $KFeF_3$ also support this expectation.

We have investigated the electron density distributions in a series of KMF_3 compounds. We can conclude from these studies that the X-ray diffraction technique can distinguish at least the spin states of the first-series transition-metal elements when they are contained in crystals with simple structures.

* See deposition footnote.

The authors wish to express their sincere gratitude to Professor A. Ito of Ochanomizu University for kindly supplying the crystal specimen. We are indebted to Dr M. Sano, Dr E. Miyoshi and Professor H. Kashiwagi for supplying the program *JGRAPH*. Our thanks are also due to Mr N. Kijima who wrote the program *FRPLOT* on the basis of *JGRAPH*. All the difference Fourier maps were depicted by *FRPLOT*. Part of the cost was met by a Grant-in-Aid for Scientific Research, No. 56420019, from The Ministry of Education, Science and Culture, to which the authors' thanks are due.

References

BOND, W. L. (1951). *Rev. Sci. Instrum.* **22**, 344.

International Tables for X-ray Crystallography (1967). Vol. II, 2nd ed. Birmingham: Kynoch Press.

International Tables for X-ray Crystallography (1974). Vol. IV. Birmingham: Kynoch Press.

IWATA, M. & SAITO, Y. (1973). *Acta Cryst.* B**29**, 822–832.

KIJIMA, N., TANAKA, K. & MARUMO, F. (1981). *Acta Cryst.* B**37**, 545–548.

KIJIMA, N., TANAKA, K. & MARUMO, F. (1983). To be published.

MACHIN, D. J., MARTIN, R. L. & NYHOLM, R. S. (1963). *J. Chem. Soc.* pp. 1490–1500.

MARUMO, F., ISOBE, M. & AKIMOTO, S. (1977). *Acta Cryst.* B**33**, 713–716.

MARUMO, F., ISOBE, M., SAITO, Y., YAGI, T. & AKIMOTO, S. (1974). *Acta Cryst.* B**30**, 1904–1906.

TANAKA, K., KONISHI, M. & MARUMO, F. (1979). *Acta Cryst.* B**35**, 1303–1308.

TANAKA, K., KONISHI, M. & MARUMO, F. (1980). *Acta Cryst.* B**36**, 1264.

TORIUMI, K., OZIMA, M., AKAOGI, M. & SAITO, Y. (1978). *Acta Cryst.* B**34**, 1093–1096.

Acta Cryst. (1983). B**39**, 564–569

Charge-Density Distribution in Crystals of $CuAlO_2$ with *d–s* Hybridization

BY T. ISHIGURO, N. ISHIZAWA, N. MIZUTANI AND M. KATO

Department of Inorganic Materials, Tokyo Institute of Technology, O-okayama, Meguro-ku, Tokyo 152, *Japan*

AND K. TANAKA AND F. MARUMO*

The Research Laboratory of Engineering Materials, Tokyo Institute of Technology, Nagatsuta, Midori-ku, Yokohama 227, *Japan*

(*Received* 3 *March* 1983; *accepted* 5 *May* 1983)

Abstract

The electron-density distribution in crystals of $CuAlO_2$ was investigated on the basis of X-ray intensity data collected by single-crystal diffractometry. The crystal has a delafossite $CuFeO_2$ structure, containing the Cu^+ ion with linear twofold coordination. Several peaks observed on the difference Fourier maps after the spherical-atom refinement were well explained by assuming aspherical scattering factors of electrons in

* To whom correspondence should be addressed.

0108-7681/83/050564-06$01.50

the *d–s*-hybridized orbital and anharmonic thermal vibration of the Cu^+ ion. [Crystal data: rhombohedral, $R\bar{3}m$, $a = 2{\cdot}8567\,(1)$, $c = 16{\cdot}943\,(1)$ Å, $V = 119{\cdot}74\,(1)$ Å^3, $Z = 3$, $D_x = 5{\cdot}12$, $D_m = 5{\cdot}06$ Mg m^{-3}, μ(Mo $K\alpha$) = 13·81 mm^{-1}.]

Introduction

The d^{10} ions such as Cu^+, Ag^+, Au^+ or Hg^{2+} have filled *d* orbitals and, therefore, spherical electron-density distributions are expected for these ions. However, Orgel (1966) proposed the *d–s*-hybridized orbital model for d^{10} ions with linear twofold coordinations (*e.g.* Cu^+ in cuprite, Cu_2O). As the energy difference between 3*d* and 4*s* orbitals is small, the $3d_{z^2}$ orbital whose lobes extend toward the ligands can hybridize with the empty 4*s* orbital to form hybridized orbitals $1/\sqrt{2}(d_{z^2} - s)$ and $1/\sqrt{2}(d_{z^2} + s)$. One of the orbitals, $1/\sqrt{2}(d_{z^2} - s)$, has no lobe in the direction of the ligands so that the linear coordination can be stabilized by the aspherical electron configuration with empty $1/\sqrt{2}(d_{z^2} + s)$ and filled $1/\sqrt{2}(d_{z^2} - s)$ orbitals.

Delafossite $CuFeO_2$-type compounds with formula $A^+B^{3+}O_2$ have a very anisotropic structure (Fig. 1). It is constructed by the alternate stacking of edge-shared $\{BO_2^-\}_\infty$ octahedral layers and A^+-ion layers perpendicular to the *c* axis. Each A^+ ion is coordinated linearly by two O^{2-} ions. The A^+ ion is restricted to a d^{10} or a d^9 ion, while many trivalent cations can enter into the octahedral site. Rogers, Shannon, Prewitt & Gillson (1971) ascribed the anisotropic electrical conductivity of the delafossite-type compounds to the *d–s* hybridization of the A^+ ions. Electrons can transfer *via* the overlap between the $1/\sqrt{2}(d_{z^2} - s)$ non-bonding orbitals of the A^+ ions. On the other hand, the $1/\sqrt{2}(d_{z^2} + s)$ orbital is used for bonding to the O^{2-} ions.

Spatial distributions of *d* electrons have been investigated in many crystals of transition-metal compounds by calculating deformation-density maps. Recently, the electron populations in the *d* orbitals were refined for several crystals using aspherical scattering factors or multipole density functions; *e.g.* $[Co(NH_3)_6][Cr(CN)_6]$ (Iwata, 1977) and $KCuF_3$ (Tanaka, Konishi & Marumo, 1979) for the former, and FeS_2 (Stevens & Coppens, 1979) for the latter. Tanaka *et al.* (1979) studied the electron-density distribution in crystals of $KCuF_3$ with Jahn–Teller distortion by the X-ray diffraction method. Residual $3d$-electron peaks around the Cu^{2+} ion on the difference Fourier maps were well explained with aspherical scattering factors for the Cu^{2+} ions by assuming linear combination of the wavefunctions: $\Psi_g = \cos(\varphi/2)d_{z^2} + \sin(\varphi/2)d_{x^2-y^2}$ and $\Psi_e = \sin(\varphi/2)d_{z^2} - \cos(\varphi/2)d_{x^2-y^2}$, and assuming Ψ_g and Ψ_e to be doubly and singly occupied, respectively. The value obtained for $\cos(\varphi/2)$ was 0·908, in agreement with the theoretically estimated value of Kadota, Yamada, Yoneyama & Hirakawa (1967).

For some of the transition-metal compounds, however, it is necessary to consider the *s*- and *p*-orbital contributions or the *d–s* and *d–p* hybridizations. Martin, Rees & Mitschler (1982) studied the charge-density distribution in $Mn_2(CO)_{10}$ from the X-ray diffraction data and refined the electron populations in the 4*s* orbital of Mn by the least-squares method for the first time. They obtained the electron configuration $3d^{5\cdot25}4s^{2\cdot34}$, but the value of the 4*s* population is incorrect, because it exceeds the maximum population. No trial has been reported which deals with the charge-density distributions of transition-metal compounds by taking into account hybridization schemes.

The present study shows that the deformation of the electron-density distribution in crystals of $CuAlO_2$ is well explained by assuming *d–s* hybridization with linear combination of the $3d_{z^2}$ and 4*s* orbitals for the valence electrons of the Cu^+ ion.

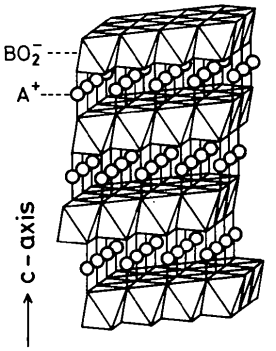

Fig. 1. Schematic view of the delafossite structure ABO_2 (3*R*), showing the linkage of the BO_6 octahedra.

Experimental

Polycrystalline $CuAlO_2$ was prepared by solid-state reaction of Cu_2O and Al_2O_3 at 1373 K in N_2 atmosphere. The cell dimensions were determined by least-squares procedure from high-angle powder X-ray diffraction data measured at 293 K using Cu $K\alpha$ radiation; these dimensions are given in the *Abstract* together with other crystal data, which agree well with previous values (Ishiguro, Kitazawa, Mizutani & Kato, 1981; Ishiguro, Ishizawa, Mizutani & Kato, 1982). D_m was measured by a pycnometer.

Single crystals of $CuAlO_2$ were grown by the slow cooling of a molten mixture of Cu_2O and Al_2O_3 from 1473 to 1323 K under atmospheric pressure. A small crystal with octahedral morphology was shaped into a sphere 0·14 mm in diameter by Bond's (1951) method. The crystal was mounted on a Philips PW 1100 automated four-circle diffractometer after it was

confirmed to be a single crystal with Buerger precession photographs. Intensities were collected [ω–2θ scan, scan speed $4°(2\theta)$ min^{-1}] in full reciprocal space within 160° in 2θ with graphite-monochromated Mo $K\alpha$ radiation in order to correct for anisotropic-extinction effects. The intensities of high-angle reflexions whose 2θ's were above 136° were measured with the setting $\varphi = 90°$. Background counts were measured at both ends of the scan range for each reflexion and the counting time was varied in proportion to the peak-scanning time and to the square root of the ratio of the background-to-peak intensity according to the standard background-measuring mode of the diffractometer. When the peak intensity exceeded 80 000 counts s^{-1}, a Ni-foil attenuator was inserted automatically to avoid a counting loss. Scanning was repeated until the total counts were more than 40 000 (maximum number of repetitions: 10).

The intensities of three standard reflexions were measured every 2 h to check the stability of the incident beam and any crystal deterioration; a small fluctuation was observed but no systematic change was detected.

Corrections for Lp and absorption factors were performed and the mean path length was calculated for each reflexion in view of the extinction correction. Weak reflexions with $|F| < 3\sigma(|F|)$ were excluded from the data set, where $\sigma(|F|)$ is the standard deviation of the observed structure amplitude due to counting statistics (3347 reflexions measured, 3284 used).

Refinement

Three kinds of least-squares refinements were carried out by changing the electron-configuration and thermal-vibration models for the Cu^+ ion in the calculation of the scattering and temperature factors. In the first step, the usual spherical scattering factors of free ions were employed for all the constituent atoms. In the second step, aspherical scattering factors were adopted for the Cu^+ ion by assuming partially hybridized orbitals. In the third step, anharmonic vibration of the Cu^+ ion was taken into account according to the generalized Willis treatment (Willis, 1969; Tanaka & Marumo, 1983). Since some of the Cu^+ ions were supposed to have been oxidized to Cu^{2+}, the chemical formula $Cu^{I}_{1-2p}Cu^{II}_{p}AlO_2$ was assumed for the crystal examined at all steps, and p was refined together with other parameters. In the first two steps, refinements were carried out by using all the reflexions in full reciprocal space, and then R values and difference Fourier maps were calculated after averaging the F_o and F_c data over symmetry-related reflexions. In the third-step refinement, only independent reflexions in $h, k, l \geq 0$ space were used, because of the restriction of the size of the computer used.

(*a*) *Refinement with spherical scattering factors*

The atomic parameters reported previously (Ishiguro *et al.*, 1981) were used for the starting values of the full-matrix least-squares refinement. Atomic scattering and dispersion-correction factors were taken from *International Tables for X-ray Crystallography* (1974) for Cu^+, Cu^{2+}, and Al^{3+}, and from Tokonami (1965) for the O^{2-} ion. In this structure, the positional parameter to be determined is only the z coordinate of the O^{2-} ion. The refinement was carried out with a modified version of *LINEX* including an extinction correction after Becker & Coppens (1974*a*,*b*, 1975). The refinement with an anisotropic type I extinction correction with a Gaussian mosaic-spread distribution gave a better R value (0·011) than that (0·014) based on type II. The refined structure parameters are listed in Table 1.

(*b*) *Refinement assuming d–s hybridization*

As suggested by Orgel (1966) and Rogers *et al.* (1971), the linear twofold coordination of a Cu^+ ion can be explained qualitatively by assuming *d–s*-hybridized orbitals,

$$\Psi_{d-s} = 1/\sqrt{2}(d_{z^2} - s) \quad \text{and} \quad \Psi_{d+s} = 1/\sqrt{2}(d_{z^2} + s),$$

where the c axis of the crystal is taken as the quantization axis z. In this refinement the degree of 4*s* contribution was determined by assuming a fully occupied orbital

$$\Psi_{d-ks} = 1/\sqrt{1+k^2}\,(d_{z^2} - ks)$$

and a non-occupied one

Table 1. *Positional parameters* ($\times 10^5$), *population p of the vacancy at the* Cu *site* ($\times 10^3$), *anisotropic temperature factors* ($\times 10^5$ Å^2), *the coefficient k* ($\times 10^2$) *and anisotropic extinction parameters* G_{ij} ($\times 10^4$) *in steps* (*a*) *and* (*b*)

The atomic positions are (0,0,0) for Cu, (0,0,0·5) for Al and (0,0,*z*) for O. The anisotropic temperature factor is defined in the form

$$\exp\{-2\pi^2[(h^2 + hk + k^2)a^{*2}U_{11} + l^2c^{*2}U_{33}]\}.$$

Refinement		(*a*)	(*b*)
Cu	p	15 (2)	17 (2)
	U_{11}	899 (2)	870 (2)
	U_{33}	345 (2)	324 (2)
	k	–	25 (2)
Al	U_{11}	317 (4)	309 (3)
	U_{33}	431 (5)	424 (5)
O	z	10977 (2)	10977 (2)
	U_{11}	531 (5)	523 (4)
	U_{33}	444 (6)	437 (6)
	G_{11}	71 (4)	61 (3)
	G_{22}	65 (2)	60 (2)
	G_{33}	85 (4)	77 (4)
	G_{12}	−15 (2)	−18 (2)
	G_{13}	5 (2)	5 (2)
	G_{23}	−7 (2)	−3 (2)
R value		0·0110	0·0101

$$\Psi_{d+ks} = 1/\sqrt{1+k^2}\,(d_{z^2} + ks),$$

where k is the parameter indicating the degree of 4s contribution. Since the Cu^+ ion is placed in a trigonal field with site symmetry $\bar{3}m$ in this structure, the fivefold-degenerate 3d orbitals split into three levels: a_g, $e_g(t_{2g})$ and $e_g(e_g)$. Here, the a_g orbital is identical to the d_{z^2} orbital. Consequently, the electronic configuration of the Cu^+ ion in this crystal is expressed by the combination of the Ar core and the fully occupied valence orbitals, $e_g(t_{2g})$, $e_g(e_g)$ and Ψ_{d-ks}.

The scattering factor for the Ψ_{d-ks} orbital can be expressed in the form,

$$f_{d-ks} = 1/(1+k^2)(f_{d_{z^2}} + k^2 f_s - 2kf_{d_{z^2},s}),$$

where $f_{d_{z^2}}$, f_s and $f_{d_{z^2},s}$ are the scattering factors for the $3d_{z^2}$ and 4s orbitals, and for the orbital product of $3d_{z^2}$ and 4s, respectively. The expressions for the scattering factors for d_{z^2}, $e_g(t_{2g})$ and $e_g(e_g)$ of the 3d transition metals with site symmetry $\bar{3}m$ were given by Iwata (1977), and the value for the 4s orbital of the Cu atom calculated by Fukamachi (1971) was used for f_s. The scattering factors of the Ar core and the orbital product of $3d_{z^2}$ and 4s are

$$f_{Ar} = f_{Cu^+} - 10\langle j_0\rangle$$

$$f_{d_{z^2},s} = -\sqrt{5}/2(3\cos^2\beta - 1)\langle j_2\rangle_{ds},$$

where β is the angular coordinate of the scattering vector and the values of $\langle j_n\rangle$ are calculated with Clementi's (1965) wave function by numerical integration. The explicit form of $\langle j_n\rangle_{ds}$ is given in the Appendix.

The least-squares calculations were performed with the program *LINKT*78 written by one of the authors (KT). The refinement significantly reduced the R value to 0·0101, giving a value of 0·25 (2) for the coefficient k. The final values of the refined parameters are given in Table 1.*

(*c*) *Refinement assuming anharmonic vibration*

Anharmonic thermal vibration of the Cu^+ ion was calculated following the generalized Willis method. The vibration of the Cu^+ ion at a point with site symmetry $\bar{3}m$ is described as a motion in a potential of the following form, when the terms higher than fourth order can be neglected.

$$\begin{aligned} V(\mathbf{u}) = V_0 &+ 1/2(b_1u_1^2 + b_2u_2^2 + b_3u_3^2) + q_{1111}u_1^4 \\ &+ q_{1122}u_1^2u_2^2 + q_{2222}u_2^4 + q_{1133}u_1^2u_3^2 \\ &+ q_{2233}u_2^2u_3^2 + q_{3333}u_3^4 + q_{1123}u_1^2u_2u_3 \\ &+ q_{2223}u_2^3u_3, \end{aligned}$$

* A list of structure factors has been deposited with the British Library Lending Division as Supplementary Publication No. SUP 38573 (3 pp.). Copies may be obtained through The Executive Secretary, International Union of Crystallography, 5 Abbey Square, Chester CH1 2HU, England.

Table 2. *Harmonic* ($\times 10^{-19}$ J Å^{-2}) *and anharmonic* ($\times 10^{-19}$ J Å^{-4}) *potential parameters of the* Cu^+ *ion*

b_1	4·65 (0·01)	q_{1111}	−2·2 (1·2)
b_2	4·65 (0·01)	q_{1122}	−4·3 (2·4)
b_3	12·47 (0·09)	q_{1133}	18·8 (23·1)
		q_{2222}	−2·2 (1·2)
		q_{2233}	18·8 (23·1)
		q_{3333}	−34·9 (19·6)
		q_{1123}	−19·8 (22·2)
		q_{2223}	6·6 (7·4)

with $b_1 = b_2$, $q_{1111} = 1/2q_{1122} = q_{2222}$, $q_{1133} = q_{2233}$, and $q_{1123} = -3q_{2223}$. Here $\mathbf{u} = (u_1,u_2,u_3)$ is the displacement vector from the equilibrium position, V_0 is the potential when the atom is at rest, and the b_i's and q_{iijk}'s are the harmonic and fourth-order anharmonic potential parameters, respectively.

The refinement was performed for the independent reflexion data (h, k, $l \geq 0$) using *LINKT*80 written by one of the authors (KT). The anharmonic parameters $Q_{iijk} = (q_{iijk}/kT)$ were refined by fixing all other parameters except the scale factor, because of severe correlations between harmonic and anharmonic temperature factors. The refined anharmonic potential parameters are given in Table 2.

Results and discussion

The difference Fourier maps on the planes $z = 0$ and $y = 0$ containing the Cu^+ ion are illustrated in Figs. 2 and 3 at all steps of the refinement. On the deformation-density maps after the refinement with spherical scattering factors, a large negative peak with a depth of −0·7 e Å^{-3} is observed on the Cu–O bond at 0·45 Å from the Cu^+ ion (Fig. 2*b*), while on the plane $z = 0$ (Fig. 2*a*) a circular positive region with a maximum height of 0·3 e Å^{-3} (at 0·23 Å from Cu^+) surrounds the Cu^+ ion, and a negative region with a maximum depth of −0·4 e Å^{-3} (at 0·49 Å from Cu^+ on the Cu–Cu bonds) is observed outside the positive region. Further, positive peaks with heights of 0·4 e Å^{-3} lie at 0·71 Å from Cu^+ on the lines bisecting the angles between two neighbouring Cu–Cu bonds. These features roughly agree with Orgel's electron-configuration model of the *d–s* hybridization. The negative peaks on the Cu–O bonds and the circular positive region on the plane $z = 0$ disappeared on the maps (Fig. 3) after the refinement with the assumption of the aspherical scattering factor for the Cu^+ ion. However, the positive and negative isolated peaks on the plane $z = 0$ did not vanish, though they are reduced in magnitude, and new positive peaks appeared with height 0·3 e Å^{-3} on the Cu–O bonds at 0·30 Å from the Cu^+ ion. All of these peaks completely disappeared after the refinement assuming anharmonic vibration of the Cu^+ ion.

The k value of 0·25 (2) which was obtained gave partially hybridized valence orbital $0{\cdot}97d_{z^2} - 0{\cdot}24s$ for

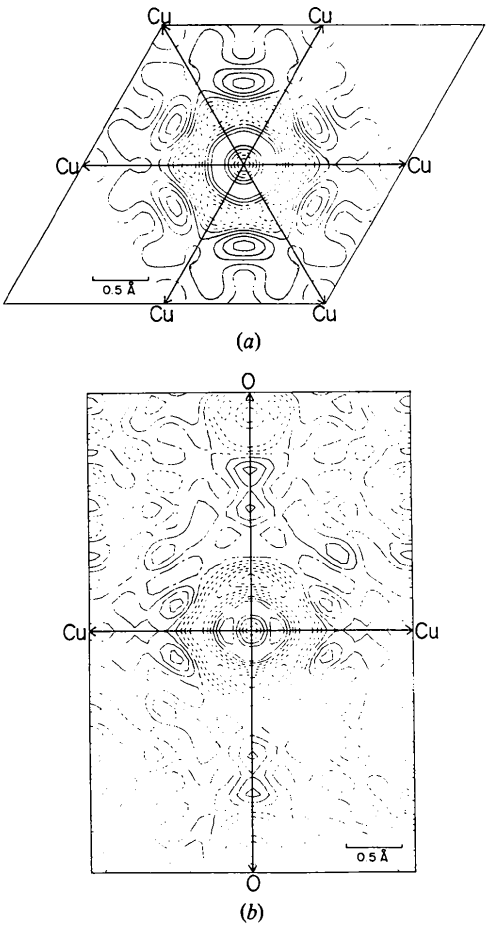

Fig. 2. The sections of the difference Fourier maps, (*a*) $z = 0$ and (*b*) $y = 0$ planes, after the refinement with the spherical scattering factors. Contours are at intervals of 0·1 e Å^{-3}. Negative and zero contours are in broken and long-dash/short-dash lines, respectively.

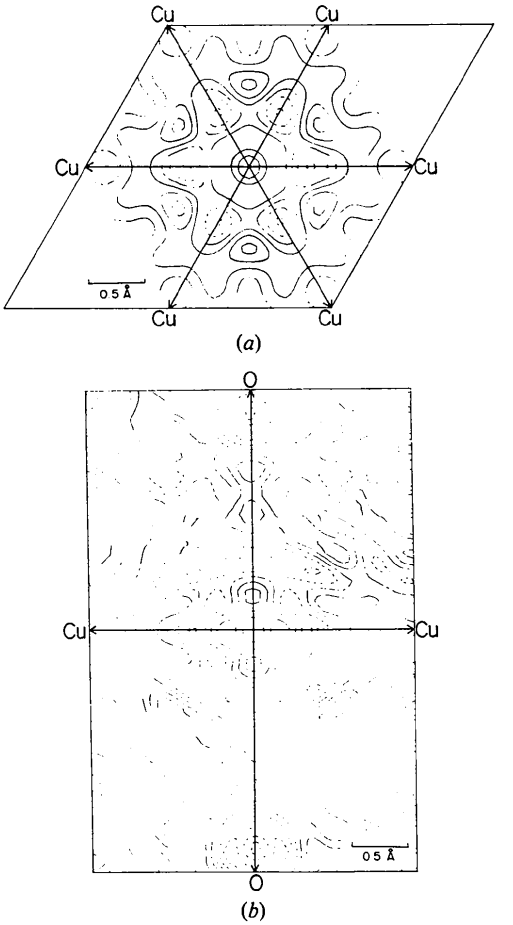

Fig. 3. The sections of the difference Fourier maps, (*a*) $z = 0$ and (*b*) $y = 0$ planes, after the refinement assuming *d*–*s* hybridization. Contours are at intervals of 0·1 e Å^{-3}. Negative and zero contours are in broken and long-dash/short-dash lines, respectively.

the Cu^+ ion. The assumption of the hybridization model by Orgel, which corresponds to $k = 1$, gave large positive peaks on the Cu–O bonds. Thus, the electron configuration of the Cu^+ ion in $CuAlO_2$ crystals was not given exactly by Orgel's model, but was given by this partially hybridized model.

The fourth-order anharmonic potential V_q on the plane $y = 0$ is given by

$$(V_q)_{y=0} = -2{\cdot}2u_1^4 + 18{\cdot}8u_1^2u_3^2 - 34{\cdot}9u_3^4 \quad (\times 10^{-19}\ \text{J Å}^{-4}).$$

It takes a minimum along the Cu–O bond, which is in conformity with the appearance of a positive peak with height 0·3 e Å^{-3} on the Cu–O bond in Fig. 3(*b*). The result indicates the preferential anharmonic vibration of the Cu^+ ion along the Cu–O bond in the attractive Coulombic forces. The feature is the same as that observed on the vibration mode of the Cu^{2+} ion in $KCuF_3$ (Tanaka & Marumo, 1982). Thus, such a preferential anharmonic vibration might be generally expected in the attractive force field in an ionic crystal.

Computations were carried out on the M-200H and M-180H computers at the Computer Center of Tokyo Institute of Technology.

APPENDIX

The orbital scattering factor $\langle j_n \rangle_{ds}$ ($n = 2, 4$) is defined as

$$\langle j_n \rangle_{ds} = \int_0^\infty R_{3d}(r)R_{4s}(r)j_n(sr)r^2\,dr,$$

where $R_{3d}(r)$ and $R_{4s}(r)$ are the radial functions for the 3*d* and 4*s* orbitals of Cu^+ ions, and s is $\sin\theta/\lambda$. The explicit form of $\langle j_n \rangle_{ds}$ is given in terms of Slater-type orbitals as

$$\langle j_n \rangle_{ds} = \sum_p \sum_{p'} [(C_{3d})_p (C_{4s})_{p'} (2n_{3d})_p!]^{-1/2} \times [(2n_{4s})_{p'}!]^{-1/2} [(2\zeta_{3d})_p]^{(n_{3d})_p + 1/2} \times [(2\zeta_{4s})_{p'}]^{(n_{4s})_{p'} + 1/2} \int_0^\infty r^{(n_{3d})_p + (n_{4s})_{p'} - 2} \times \exp\{-[(\zeta_{3d})_p + (\zeta_{4s})_{p'}]r\} j_n(sr) r^2 dr,$$

where the constants $(n_{3d})_p$, $(\zeta_{3d})_p$, $(C_{3d})_p$, $(n_{4s})_{p'}$, $(\zeta_{4s})_{p'}$ and $(C_{4s})_{p'}$ are given by Clementi (1965), and $j_n(sr)$ is the nth-order spherical Bessel function. Since the 4s orbital wavefunction of Cu^+ ions is not given in Clementi's table, that of the neutral Cu atom with the electronic configuration $(1s)^2(2s)^2(2p)^6(3s)^2(3p)^6(3d)^{10}(4s)^1$ was employed in the present study.

References

BECKER, P. J. & COPPENS, P. (1974*a*). *Acta Cryst.* A**30**, 129–147.
BECKER, P. J. & COPPENS, P. (1974*b*). *Acta Cryst.* A**30**, 148–153.
BECKER, P. J. & COPPENS, P. (1975). *Acta Cryst.* A**31**, 417–425.
BOND, W. L. (1951). *Rev. Sci. Instrum.* **22**, 344.
CLEMENTI, E. (1965). *Tables of Atomic Functions.* Supplement to *IBM J. Res. Dev.* **9**, 2–19.
FUKAMACHI, T. (1971). *Tech. Rep. Inst. Solid State Phys.* B**12**, 20.
International Tables for X-ray Crystallography (1974). Vol. IV. Birmingham: Kynoch Press.
ISHIGURO, T., ISHIZAWA, N., MIZUTANI, N. & KATO, M. (1982). *J. Solid State Chem.* **41**, 132–137.
ISHIGURO, T., KITAZAWA, A., MIZUTANI, N. & KATO, M. (1981). *J. Solid State Chem.* **40**, 170–174.
IWATA, M. (1977). *Acta Cryst.* B**33**, 59–69.
KADOTA, S., YAMADA, I., YONEYAMA, S. & HIRAKAWA, K. (1967). *J. Phys. Soc. Jpn*, **23**, 751–756.
MARTIN, M., REES, B. & MITSCHLER, A. (1982). *Acta Cryst.* B**38**, 6–15.
ORGEL, L. E. (1966). *An Introduction to Transition-Metal Chemistry: Ligand-Field Theory*, 2nd. ed. London: Methuen.
ROGERS, D. B., SHANNON, R. D., PREWITT, C. T. & GILLSON, J. L. (1971). *Inorg. Chem.* **10**, 723–727.
STEVENS, E. D. & COPPENS, P. (1979). *Acta Cryst.* A**35**, 536–539.
TANAKA, K., KONISHI, M. & MARUMO, F. (1979). *Acta Cryst.* B**35**, 1303–1308; *errata: Acta Cryst.* (1980). B**36**, 1264.
TANAKA, K. & MARUMO, F. (1982). *Acta Cryst.* B**38**, 1422–1427.
TANAKA, K. & MARUMO, F. (1983). *Acta Cryst.* A**39**, 631–641.
TOKONAMI, M. (1965). *Acta Cryst.* **19**, 486.
WILLIS, B. T. M. (1969). *Acta Cryst.* A**25**, 277–300.

Acta Cryst. (1983). B**39**, 569–575

On the Non-Stoichiometric Ytterbium Sulphide Phase 'Yb_3S_4'

BY CARLOS OTERO DIAZ AND B. G. HYDE

Research School of Chemistry, Australian National University, GPO Box 4, Canberra, ACT 2601, Australia

(*Received* 10 *March* 1983; *accepted* 11 *April* 1983)

Abstract

Examination of ytterbium sulphides in the composition range $YbS_{1.34}$ to $YbS_{1.42}$ by electron diffraction reveals that this is not, as previously reported, a homogeneous solid-solution region with the **Yb_3S_4**-type structure. In addition to reflections characteristic of this structure there are satellite reflections which indicate a long-range modulation with a variable periodicity of approximately seven to eight times. This is confirmed by electron microscopy, the most obvious modulation direction being close to ⟨830⟩ of the **Yb_3S_4** subcell.

Introduction

With the passage of time, the number of crystalline 'homogeneous solid solutions' has decreased remarkably. On closer scrutiny, many have been resolved into sequences of closely spaced or even contiguous phases, each with a highly ordered structure derived from a simple prototype by one of a few crystallographic operations (*e.g.* Andersson & Hyde, 1982, and references therein). Others exhibit short-range order, and eventually decompose into phase mixtures (*e.g.* Bakker & Plug, 1981). Some achieve partial long-range order in the form of modulated structures, the modulation being often incommensurate with the unit cell of the prototype structure (*e.g.* Makovicky & Hyde, 1981; Yamamoto & Nakazawa, 1982; McLaren, 1978).

But there is still a residuum of phases with apparently random arrays of point defects and these also demand close scrutiny, particularly by techniques that are more sensitive than the more traditional methods such as X-ray diffraction. Perhaps the most powerful of these techniques is electron microscopy/diffraction, which has proved so successful in some of the cases already referred to. Here we will report on such a study of the phase based on Yb_3S_4.

Flahaut and co-workers reported this phase as having a continuous range of homogeneous solid

0108-7681/83/050569-07$01.50